Title: Regional activity in the rat anterior cingulate cortex and insula during persistence and quitting in a physical-effort task

Abbreviated Title: Cingulate & insula activity during an effort task

Blake S. Porter, Kunling Li, and Kristin L. Hillman

Department of Psychology

Brain Health Research Centre

University of Otago

275 Leith Walk, Dunedin 9016, New Zealand

Corresponding Author: Blake S. Porter, blakeporterneuro@gmail.com

Pages: 36

Figures: 8

Tables: 0

Word count Abstract: 250

Word count Introduction: 628

Word count Discussion: 1483

Conflict of Interest: The authors declare no competing financial interests.

Acknowledgments: This study was supported by Marsden Fund grant U001617 (K.L.H.) from the Royal Society of New Zealand Te Apārangi.

Abstract

As animals carry out behaviors, particularly costly ones, they must constantly assess whether or not to persist in the behavior or quit. The anterior cingulate cortex (ACC) has been shown to assess the value of behaviors and to be especially sensitive to physical effort costs. Complimentary to these functions, the insula is thought to represent the internal state of the animal including factors such as hunger, thirst, and fatigue. Utilizing a novel weight lifting task for rats, we characterized the local field potential (LFP) activity of the ACC and anterior insula (AI) during effort expenditure. In the task male rats are challenged to work for sucrose reward, which costs progressively more effort over time to obtain. Rats are able to quit the task at any point. We found modest shifts in LFP theta (7-9 Hz) activity as the task got progressively more difficult in terms of absolute effort expenditure. However, when the LFP data were analyzed based on the rat's relative progress towards quitting the task, or performance state, substantial shifts in LFP power in the theta and gamma (55-100 Hz) frequency bands were observed in ACC and AI. Both ACC and AI theta power decreased as the rats got closer to quitting, while ACC and AI gamma power increased. Furthermore, coherency between ACC and AI in the delta (2-4 Hz) range shifted alongside the rat's performance state. Overall we show that ACC and AI LFP activity changes are reflective of the rats' relative performance state in an effort-based task.

Significance Statement

Animals need to assess whether or not a behavior is worth pursuing based on their internal states (e.g., hunger, thirst, fatigue) and the costs and benefits of the behavior. However, internal states often change as behaviors are carried out, such as becoming satiated or tired, necessitating constant reassessment as to whether to continue the behavior or quit. We characterized brain activity in two cortical regions, the anterior cingulate cortex and insula, as rats carried out a progressively challenging physical-effort task. Both brain regions showed significant shifts in activity as the rats approached their quitting point. Our study provides one of the first characterizations of neural activity changes as an animal approaches the decision to quit an effortful task.

Introduction

When tasks become effortful, animals must evaluate whether additional physical and/or mental effort expenditures are worthwhile. This evaluation requires both a cost-benefit assessment of the task and an interoceptive assessment – an animal must gauge physiological and/or psychological preparedness to handle any continued effort expenditure. While multiple brain regions are involved in these processes, two regions appear central: the anterior cingulate cortex (ACC) and the anterior insula (AI).

Based on lesion and electrophysiological studies, the ACC is implicated in effort-based cost-benefit analysis. For example, when rats are presented behavioral options that include varying levels of effort, ACC single unit activity is reflective of the available behavior with highest utility (Hillman and Bilkey 2010; Cowen et al. 2012; Hart et al. 2019; Porter et al. 2019). Ensembles of neurons in rat ACC have also been shown to track an animal's successful progression through a behavioral choice task (Lapish et al. 2008). Human EEG recordings indicate that frontal midline theta, thought to originate from the ACC, correlates to task effort and difficulty (Smit et al. 2005; Cavanagh and Frank 2014). Taken together, heightened population activity in the ACC may help drive action towards high-utility goals when effort is required (Amiez et al. 2006; Kennerley and Wallis 2009; Cowen et al. 2012; Hillman and Bilkey 2012).

The AI is implicated in representing the interoceptive state of the body. The insula receives hypothalamic, autonomic, and visceral inputs making the AI is well-positioned to process interoceptive information on states such as hunger and pain, which can influence cost-benefit decision-making (Cechetto and Saper 1987; Craig 2003; Critchley 2005). In rats, lesions to the AI result in maladaptive persistence and perseveration behaviors in reward devaluation scenarios

(Balleine and Dickinson 2000; Parkes et al. 2015; Moschak et al. 2018). One interpretation of this is that AI functionality is needed during ongoing cost-benefit decision making to spur effort reallocation – in the form of task switching and/or quitting – when a behavior has decreased utility relative to the body's needs. In turn, the AI's interoceptive state representation could be utilized by the ACC to evaluate the costs and benefits of persisting at or quitting a behavior.

White matter tracts between the cingulate and insula have been traced in humans (Moisset et al. 2010), and resting state functional connectivity between the regions have been reported (Sridharan et al. 2008; Taylor et al. 2009). As outlined by Medford and Critchley (2010) the regions could function in tandem: the AI integrating external and internal sensory inputs to represent the current state of the organism, with the ACC then utilizing this state representation to drive relevant behaviors. If external and internal sensory inputs to the AI increasingly signal effort costs (fatigue, energy depletion), the ACC could bias behaviors away from continued energy expenditure. Both brain regions have been shown to encode the expected energetic cost of physically demanding behaviors (Prevost et al. 2010), and as tasks get increasingly effortful the ACC and AI show conjoint BOLD activation (Engstrom et al. 2014). It is not well-understood, however, how dynamic changes in conjoint ACC-AI activity correlate to changes in effortful task performance. Furthermore, few studies have examined ACC-AI activity to the point of quitting.

To address these questions directly, we recorded local field potentials (LFPs) from the ACC and AI of rats the animals performed a novel weight lifting task (WLT). The WLT allows systematic manipulation of physical effort costs while maintaining the same motor pattern, spatial context, and reward value. We predicted that low-frequency LFP power from the ACC would inversely correlate to effort costs, while low-frequency LFP power from the AI would positively correlate

to effort costs. We also aimed to characterize ACC-AI LFP activity at the quitting point, a time period that to our knowledge has been minimally investigated at the electrophysiological level.

Materials and Methods

Subjects. Male Sprague-Dawley rats (n=16, weighing 400 - 575 g at the time of experiment; Hercus Taieri Resource Unit, New Zealand) were single housed in individually ventilated cages, 38 x 30 x 35 cm (Tecniplast, Italy). Animals were maintained on a 12 h reverse light cycle, with experimentation occurring during the animals' dark, active phase. Water was available *ad libitum*. Daily chow (Teklad diet; Envigo, USA) was rationed to promote interest in food reward during experimentation. Rats were weighed twice per week and daily food rations were adjusted to maintain each animal's body weight ≥ 85% of their free-feeding body weight. All procedures were approved by the University of Otago's Animal Ethics Committee, protocol 91/17.

Training. Prior to surgery, animals were trained in the WLT as previously described (Porter and Hillman 2019). Briefly, the WLT occurs in a 120 x 90 x 60 cm arena (Figure 1a & 1b); an animal is progressively shaped to pull a rope 30 cm to trigger dispensing of 0.25 mL of 20% sucrose solution. The rope can be weighted from 0 to 225 g to increase the effort demands of the task, however only 0 g and 45 g are used in the training phase. Once an animal can perform 20 successful pulls (10 pulls on 0 g followed immediately by 10 pulls on 45 g) in under five min, they are considered trained in the WLT and ready for surgery.

Surgery. Animals were implanted with two, 200 µm insulated nichrome electrodes (Johnson Matthey PLC, UK) under isoflurane anesthesia as previously described (Porter et al. 2019). Stereotaxic coordinates, based on Paxinos and Watson (2007), were set as follows: ACC + 3.7

mm anteroposterior (AP) from Bregma, + 0.4 mm mediolateral (ML), - 1.0 mm dorsoventral (DV); and AI + 2.7 mm AP from Bregma, + 2.0 mm ML, and - 5.8 mm DV at an angle of 20° ML. All implants were in the right hemisphere. A 4 mm stainless steel screw placed over the cerebellum served as the ground connection. Five to seven additional 3 mm stainless steel screws were placed in the skull for dental cement to anchor to. Electrodes were secured with UV cure self-etching dental cement (Maxcem Elite™, Kerr Corp., USA) followed by additional self-cure dental acrylic (Lang Dental Manufacturing Company, Inc., USA) for additional strength. Ten days after surgery and post-operative care, rats were retested on the WLT with 0 and 45 g to ensure no loss of function from surgery and to check the quality of the electrophysiological signals. Within 3 days, all rats returned to baseline performance criterion (i.e., 10 successful trials on 0 g and 10 successful trials on 45 g, all within 5 min). Once criterion performance was confirmed, experimentation began.

Weight Lifting Task. To test persistent, effortful behavior, a progressive weight lifting paradigm was utilized. This paradigm has been detailed previously (Porter and Hillman 2019). Briefly, the rats need to pull a rope with a weight attached for 30 cm to trigger release of 0.25 mL of 20% sucrose solution. In the progressive WLT, an animal is challenged to pull progressively heavier weights: the weight starts at 0 g and after every 10 successful, rewarded pulls, 45 g of weight is added to the rope. The animal continues until they quit or a rope weight of 225 g is reached. If 10 successful pulls are achieved on 225 g then the weight is made ‘impossible’ by affixing it to the set-up such that the weight can only be pulled up approximately 15 cm, thus making it impossible to trigger a reward. Quitting was defined as 2 minutes of no attempted rope pulls.

Each task session was bookended with 2 min of open field exploration in the arena. During these open field periods the rope was not available and no sucrose was dispensed. The initial 2 min

exploration provided a baseline measure of LFP and locomotor activity prior to beginning the WLT. Likewise, the 2 min exploration at the end of the task provided post-task LFP and locomotor measurements. At the end of the 2 min post-task exploration, a sucrose reward check was performed to test for satiation. The sucrose satiation check entailed two manually released sucrose rewards and the rats had one minute to approach and consume the sucrose. Whether or not they approached and consumed the sucrose was noted by the experimenter.

Recordings. Local field potentials were recorded using a Neuralynx (USA) acquisition system (either a Digital Lynx SX or SX-M) at 6,400 or 5,000 Hz, respectively, with a bandpass filter set between 0.1 and 500 Hz. Rats were tethered via a Neuralynx Saturn-1 commutator to either a Neuralynx HS-36-LED or HS-36-mux-LED pre-amp headstage. Rat position was tracked via two headstage mounted LEDs by Neuralynx's Cheetah software using an overhead camera. Rats were ran in a darkened room to allow tracking of the LEDs. The Neuralynx acquisition system also recorded TTL signals from the WLT Arduino Uno microcontroller (Arduino.cc) that timestamped when the weight was lifted off the base, when the weight returned down to the base, and when the weight was successfully pulled up 30 cm and a reward was released.

Histology. At the end of the study, animals were transcardially perfused with 4% paraformaldehyde in PBS and histology performed as previously described (Porter et al. 2019). Thionin staining confirmed 13 out of 16 correct placements in the ACC (Figure 1c), and 13 out of 16 in the AI (Figure 1d). LFP data from electrodes with incorrect placements were excluded from analysis. Behavioral data was analyzed for all 16 rats.

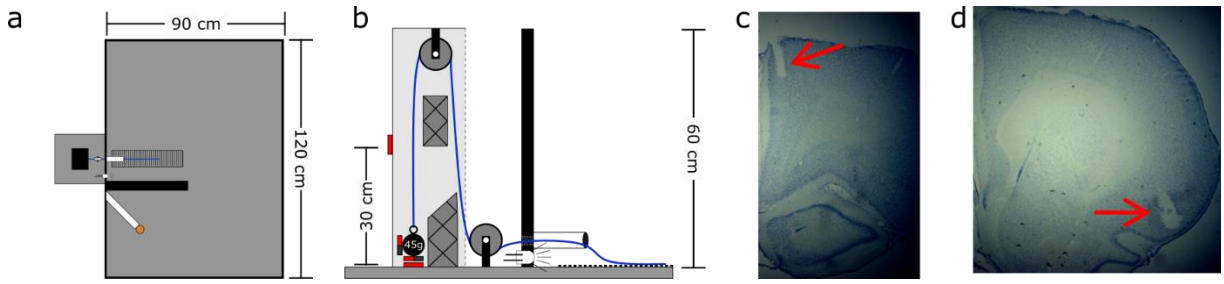

Figure 1: Experimental overview. Weight lifting task apparatus (a) and weight lifting pulley schematic (b), adopted from Porter and Hillman (2019). Example histological confirmation of electrode placements in the ACC (c) and AI (d). Red arrows indicate termination location.

Experimental Design and Statistical Analysis. Statistically analysis was carried out in MATLAB with custom and native scripts. All statistical analyses were double checked in Prism (Version 8.4.1; GraphPad Software). Behavioral and LFP data were parsed based on the timestamps relayed by the Arduino TTL signals and experimenter notes using MATLAB. Methods for behavioral analyses have been reported in detail previously (Porter and Hillman 2019). Briefly, data from a given behavioral metric was first tested for normality using a one sample Kolmogorov-Smirnov test. Depending on the data's distribution the appropriate statistical test was selected, either a one-way ANOVA or Kruskal-Wallis test, with a P value of 0.05.Dunn-Sidak's Method was used for making post-hoc multiple comparisons.

LFP analyses: Each rat (n=16) ran the progressive WLT for 5 to 8 recording sessions, one session per day. In total there were 83 recording sessions for ACC data and 82 for AI. Each recording session was broken up into epochs based on the different rope weights (0, 45, 90 g, etc.). Each epoch began when the respective weight was attached to the rope, and ended when the next weight was attached after 10 successful trials or until the rat quit. The 0 g epoch began

immediately following the 2 min pre-baseline period when the rope was extended into the apparatus. Our LFP analyses focused on rope pull attempts. LFP attempt epochs were defined as the 2 sec preceding the rat lifting the weight, i.e., the initiation of task execution. If attempts overlapped in series (e.g., the rat pulled the weight, dropped it, and then pulled again within 2 sec) only the first attempt was used. Attempts were analyzed regardless of their outcomes (successful or failed pull). If the rat did not have at least five attempts for a given weight, that weight was not included in the LFP analysis.

LFP signals were down sampled to 200 Hz prior to analysis using Matlab's downsample function. LFP data were then analyzed using the Chronux toolbox (Bokil et al. 2010). After down sampling, LFP signals were locally detrended for low frequency movement artefacts using Chronux's locdetrend function with a 500 ms moving window and 100 ms overlap. Following local detrending, 50 Hz electrical mains noise was removed with Chronux's rmlinesc function. LFP power spectrums (PSDs) and spectrograms were then calculated via the multi-taper spectral estimation method using the Chronux toolbox with a time-bandwidth product of 3 with 5 tapers, no FFT padding, and a bandpass filter of 0 to 100 Hz. The resulting power spectra covered 0 to 100 Hz in roughly 0.5 Hz increments. For a given recording session, all power spectrums and spectrograms were z-scored based on 100 randomly sampled 2 sec epochs from the pre-baseline period. Any trial where more than 15% of the frequency spectrum (0 to 48 Hz) measured over ± 3 standard deviations (SD) was removed. Likewise, trials were excluded if mean power measured over ± 3 SD within a frequency band of interest. While rare, these noisy trials tended to be caused by the rats hitting the headstage on the wall or arena floor, or from grooming behaviors prior to a pull attempt. Coherency, a measure of oscillatory synchronization, between the ACC and AI was analyzed using Chronux's coherency function. Coherency was averaged

across trials and data were pooled across sessions and rats. Spectrograms were created with Chornux's mtspecgram function using a time-bandwidth product of 3, 5 tapers, a padding factor of 1, and a 0.5 second moving window with 0.05 second step. The normalized LFP data from each trial within a weight was averaged and then data were pooled across rats and sessions.

One-way ANOVA was used to test whether normalized power within a frequency band across rope weights with a significance value of 0.05. In addition to absolute weights, we also analyzed the data in terms of the rat's relative performance state. For each individual session we assessed LFPs on: the start weight of 0g, the highest weight the rat achieved (i.e., completed 10 trials on), and the weight the rat quit on. One-way repeated measures ANOVA was used to test for changes in power and coherency across these three performance states within the session. Tukey's Honestly Significant Difference Procedure was used to test for post-hoc multiple comparisons using Matlab's multcompare function.

Our graphs attempt to show all the data points where feasible. However, we chose to programmatically limit the Y-axis based on the minimum and maximum quartiles of the data. As a result some individual data points outside of these ranges are not shown graphically. However, for coherency analyses, we hard coded the y-axis for all frequency bands for easier visual comparisons as coherency values can only range from 0 to 1.

This study was not preregistered. Data is not openly accessible but can be made available upon request.

Code Accessibility. Analysis was carried out with custom MATLAB scripts. All code is available upon request to the corresponding author.

Results

Behavioral impact of progressive WLT. We first set out to characterize how rats behaved on the progressive WLT. Sixteen rats were tested on the progressive weight paradigm for a total of 114 sessions; each rat contributed 5-8 sessions. Within a session, rats generally completed the first three weights (0, 45, and 90 g) with ease before quitting on one of the latter three weights (135, 180 or 225 g; Figure 2a). The most common quit weight was 225 g, occurring in 33% of sessions. Rats' average body weight was not correlated to the average weight they quit on ($r = 0.02$, $p = 0.93$). In 55% of sessions (51/114), rats completed at least one successful 30 cm pull on their quit weight before quitting, indicating that they were capable of successfully performing the action of lifting that weight up 30 cm but chose not to continue on. In 98% of sessions (112/114), rats were capable of at least lifting their quit weight off of the base. Together, rats' pulling behavior indicated rats likely quit the task due to the increasing effort cost caused by the increasing weight. Furthermore, in 100% of sessions rats consumed the sucrose rewards during the end-of-session satiation check, suggesting that they did not quit the rope pulling task due to sucrose satiation.

The increasing effort load of the weights had a significant impact on the rats' behavior. As the weight got progressively heavier, it took rats significantly longer to successfully pull the weight up 30 cm from the base ($H (5, 469) = 232$, $p < 0.0001$; Figure 2b). Pairwise comparisons between each weight and its preceding weight revealed significant increases in successful pull times across most weight pairs (p's < 0.02), however, pull times between 0 g and 45 g ($p = 0.06$) and 180 g and 225 g ($p = 1.0$) were similar.

The increase in successful pull time with heavier weights indicates that the heavier weights are indeed more effortful for the rats. Successful pull times, however, can only be calculated for

rewarded attempts and therefore do not fully capture the rats' persistence at the task as it becomes increasingly difficult. In order to characterize the rats' persistence we calculated an attempts-to-reward ratio of the average number of attempts made for each rewarded attempt for each weight. A ratio of 1.0 indicates every attempted pull was successful in triggering reward. Ratios greater than 1.0 indicate that the rats failed to pull the weight 30 cm on some attempts. Rats made significantly more attempts per reward as the weights increased ($H(5, 482) = 268$, $p < 0.0001$; Figure 2c). Pairwise comparisons revealed that rats generally made more attempts per reward as the weights got heavier (all p's < 0.02), however, their performance was similar between 90 and 135g ($p = 0.36$) and 180 and 225g ($p = 0.93$). Thus, as the weights increase rats fail more often to successfully lift the weight.

On 69% of sessions where rats reached the 225 g weight they were not able to complete a single successful, rewarded pull (and thus we could not compute an attempt-to-reward ratio). To get a better idea of the rats' persistence in the face of increasing effort demands, we measured the total number of attempts rats made on each weight. Weight had a significant impact on the number of attempts rats made ($H(5, 543) = 169$, $p < 0.0001$; Figure 2d). The average number of attempts increased weight-to-weight up to 180 g ($p < 0.05$), with the exception of 90 g to 135 g ($p = 1.0$). Attempts), until 225 g where attempts significantly decreased on 225g compared to 180 g ($p < 0.0001$). Overall, these behavioral metrics indicate that the progressively increasing weights are more and more difficult for the rats to lift, requiring more effort (pull time, number of attempts) and persistence (attempt-to-reward ratio).

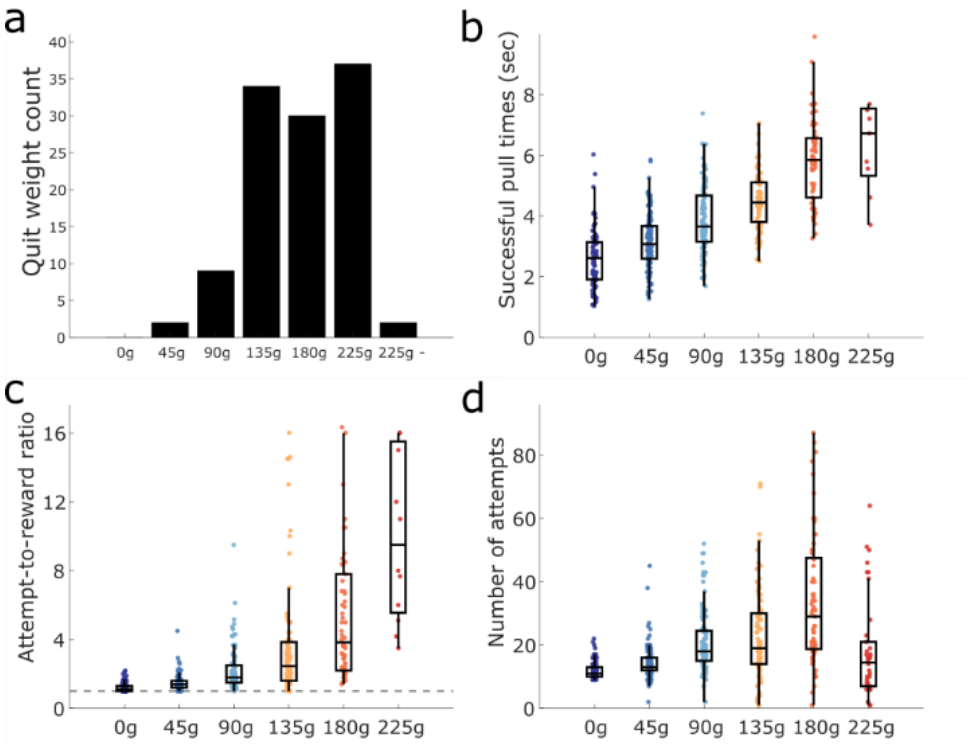

Figure 2: Progressive weight task behavior. a) Histogram of quit weight occurrence. "225g -" indicates the impossible phase where no rewards could be earned; see Methods. b) The time it took rats to pull the weights up 30 cm from the base, sufficient to trigger sucrose reward. Heavier weights took longer to lift. c) The attempt-to-reward ratio for each weight showing the average number of attempts rats made before completing a successful attempt. Dotted line represents a ratio of 1.0 where every attempt would be successful. Heavier weights took more pull attempts before a reward was successfully triggered. d) Average number of attempts rats made on each weight. Rats tended to make more attempts as weights got heavier, however, on heavier weights some rats made very few attempts before quitting.

To further ensure rats were not quitting due finishing a specific number of pulls, sucrose satiation, or time-on-task, we ran 5 rats on a modified, fixed weight version of the WLT in the week after they ran the progressive weight paradigm. Rather than the weight progressively

increasing, rats had 10 trials of 0 g followed by unlimited trials on 180 g. The 180 g weight was chosen as it was the maximal weight all 5 rats had completed 10 trials on in the progressive weight paradigm. Rats ran the fixed weight paradigm until they quit (no attempt for 2 minutes) or for one hour, whichever came first. Each rat completed 5 or 6 sessions of the fixed weight paradigm; 26 sessions were recorded in total. Compared to their progressive weight performance, during the fixed weight task the rats made significantly more attempts (median 202 attempts vs. 81 in the progressive weight; $Z = -5.11$, $p < 0.0001$; Supplemental Figure 1a), earned significantly more rewards (68 vs. 42 in the progressive weight; $Z = -4.73$, $p < 0.0001$; Supplemental Figure 1b), and performed the task for significantly longer before quitting (2123 sec vs. 1045 in the progressive weight; $Z = -4.62$, $p < 0.0001$; Supplemental Figure 1c). Overall, these data further demonstrate that rats are quitting the progressive weight task due to the increase in effort (weights) and not due to repetitive rope pulling attempts, becoming satiated on sucrose, or quitting after an elapsed time.

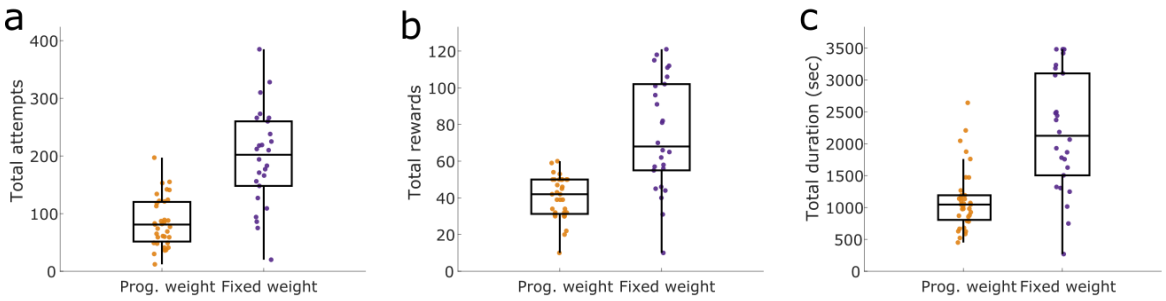

Supplemental Figure 1: Behavioral comparisons between paradigms. In the progressive weight task, 45 g of weight was added to the rope after every 10 successful pulls. In the fixed weight task, a 180 g rope weight was accessible for up to 1 hour. In the fixed weight paradigm, rats made significantly more attempts (a), earned more reward (b), and performed for longer (c), as compared to their performance in the progressive weight paradigm.

LFP correlates of progressive effort loading. We investigated the neural correlates of increasing effort costs by recording LFPs in the ACC and AI as rats carried out the progressive WLT. We specifically focused our analyses on the 2 sec prior to the rat lifting the weight up. This period reflects the rat choosing to actively engage in the task and make an attempt at expending energy to earn a reward. The average normalized ACC PSD for each weight is shown in Figure 3a. Changes in power in the delta (2-4 Hz), theta (7-9 Hz), beta (15-25 Hz), and gamma (55-100 Hz) frequency ranges were assessed. We predicted that low-frequency LFP power from the ACC would inversely correlate to effort costs, while low-frequency LFP power from the AI would positively correlate to effort costs.

The overall normalized ACC PSD for each weight is shown in Figure 3a. Weight had a significant influence on delta ($F(5, 356) = 3.22$, $p = 0.007$; Figure 3b) and theta band power ($F(5, 356) = 2.83$, $p = 0.016$; Figure 3c). Post-hoc multiple comparisons on delta power using Dunn-Sidak's test revealed a significant pairwise difference between 0g and 135 g ($p = 0.048$) while all other pairs were not significantly different (p's > 0.05). Post-hoc comparisons for theta power showed a significant decrease in power from 0g to 225 g ($p = 0.046$) while all other pairs were not significantly different (p's > 0.05). Beta ($F(5, 356) = 1.02$, $p = 0.407$; Figure 3d) and gamma ($F(5, 356) = 1.87$, $p = 0.10$; Figure 3e) power were not significantly impacted by weight.

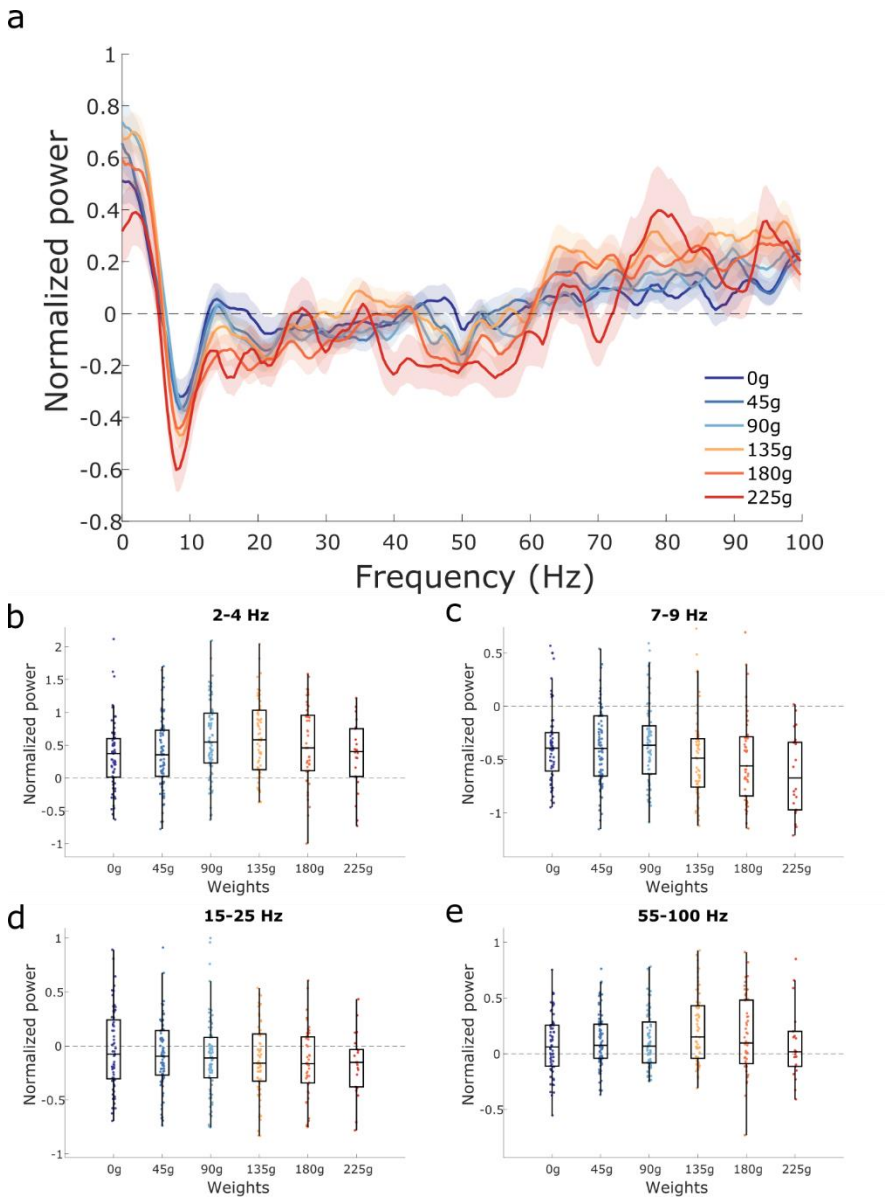

Figure 3: Changes in ACC LFP rhythms with increasing effort. a) Multi-taper power spectrum of ACC LFP across the six different weights. Shaded error bars represent ± 1 S.E.M. b-d) Normalized power across the four rhythms of interest (delta, theta, beta, and gamma, respectively). Box plots show first, second (median; middle line), and third quartiles. Whiskers are 1.5 times the interquartile range. All power calculations were normalized using the 2 min pre-baseline period, see Methods.

The overall normalized AI PSD for each weight is shown in Figure 4a. Weight had no effect on power within the delta ($F(5, 359) = 0.71$, $p = 0.61$; Figure 4b), theta ($F(5, 359) = 1.85$, $p = 0.10$; Figure 4c), or beta band ($F(5, 359) = 1.21$, $p = 0.31$; Figure 4d). Weight did have a significant effect on power within the gamma band ($F(5, 359) = 4.42$, $p < 0.0001$; Figure 4e). Post-hoc pairwise comparisons revealed significant differences between gamma power on 0 g compared to the other weights (p's < 0.05), with the exception of 45 g ($p = 0.11$) and 180 g ($p = 0.07$). No other pairwise comparisons were significant (p's > 0.05).

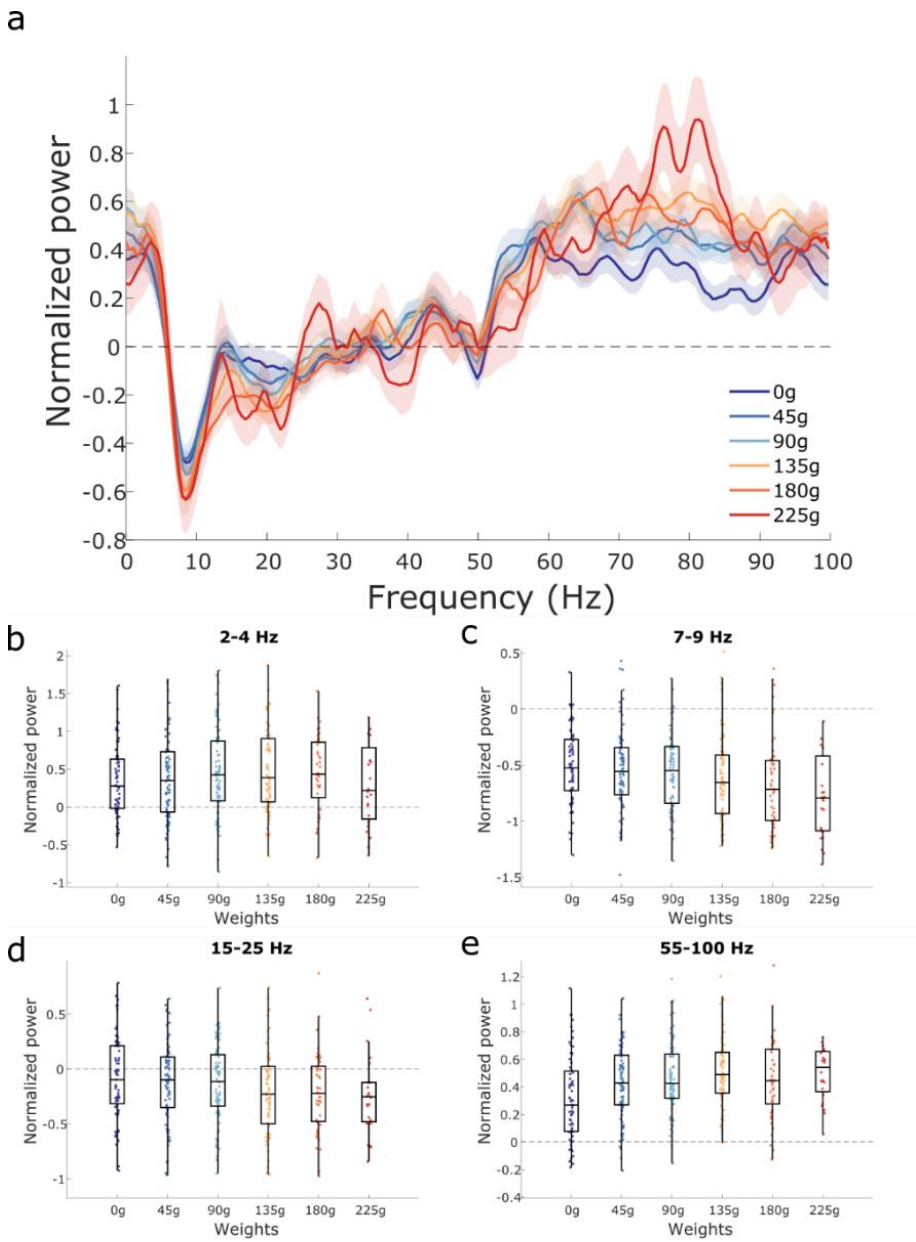

Figure 4: Changes in AI LFP rhythms with increasing effort. a) Multi-taper power spectrum of AI LFP across the six different weights. Shaded error bars represent ± 1 S.E.M. b-d) Normalized power across the four rhythms of interest (delta, theta, beta, and gamma, respectively). Box plots show first, second (median; middle line), and third quartiles. Whiskers are 1.5 times the interquartile range. All power calculations were normalized using the 2 min pre-baseline period.

LFP correlates of quitting behavior. In addition to examining how increases in effort load (weight) affected regional activity in the ACC and AI, we were interested in examining how an animal's performance state correlated to regional neural activity. As the WLT is a self-driven task, the animal can quit at any point, on any weight. This generates inter- and intra-individual variability in quit points, and quit point metrics, likely reflecting variability in motivational states. Due to the rats' quitting behaviors, the motivational state of a rat on a given weight could be different to that of another rat on the same weight. For example, one rat may quickly complete 10 successful pulls on the 135 g weight, while another rat may quit on 135 g after only a few attempts. To address session-to-session variability, we divided up the rats' performance based on their relative achievement for a given session. For each individual session we assessed LFPs from three blocks of interest: 1)We analyzed the specific frequency bands during the low-effort start weight of 0 g; 2) the rat's achievement weight (i.e., the maximum weight that the rat completed 10 trials on); and 3) the weight the rat quit on.

The overall normalized ACC PSD across the three states can be seen in Figure 5a. When each frequency band of interest was independently assessed, significant differences in power were observed between performance states in the delta rhythm ($F(1.99, 103.3) = 15.9$, $p < 0.0001$; Figure 5b), theta rhythm ($F(1.79, 93.0) = 6.05$, $p = 0.0047$; Figure 5c), beta ($F(1.61, 83.9) = 3.70$, $p = 0.038$; Figure 5d), and gamma rhythm ($F(1.59, 82.8) = 7.28$, $p = 0.0026$; Figure 5e). Post-hoc comparisons revealed a significant increase in ACC delta power between 0 g and the achievement weight ($p = 0.011$). No other pairwise comparisons reached significance (p's > 0.05).

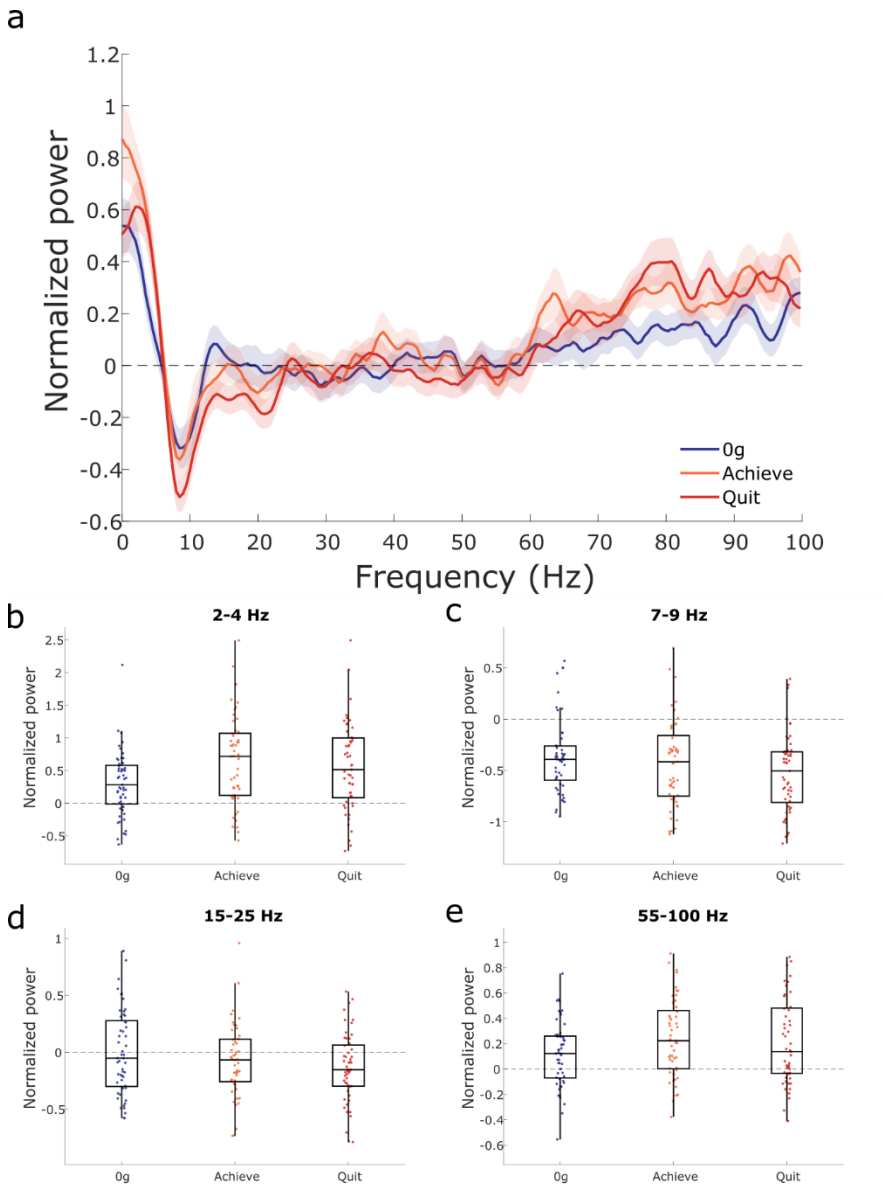

Figure 5: Changes in ACC LFP rhythms across performance states. a) Multi-taper power spectrum of ACC LFP across the three performance states. Shaded error bars are ± 1 S.E.M. b-d) Normalized power across the four rhythms of interest (delta, theta, beta, and gamma, respectively). Box plots show first, second (median; middle line), and third quartiles. Whiskers are 1.5 times the interquartile range. All power calculations were normalized using the pre-baseline period.

The overall normalized AI PSD across performance states is shown in Figure 6a. Power in the delta frequency range ($F(1.81, 97.7) = 4.0$, $p = 0.025$; Figure 6b), theta ($F(1.76, 95.0) = 17.3$, $p < 0.0001$; Figure 6c), beta ($F(1.65, 89.3) = 5.75$, $p = 0.0072$; Figure 6d), and gamma rhythms ($F(1.76, 94.9) = 19.9$, $p < 0.0001$; Figure 6e) all showed significant differences between performance states. Post-hoc pairwise tests revealed a significant decrease in theta power from 0 g to the quit weight ($p = 0.017$) while gamma power increased from both 0 g to the achievement weight ($p = 0.004$) and from 0 g to the quit weight ($p < 0.0001$). No other post-hoc pairwise comparisons were significant.

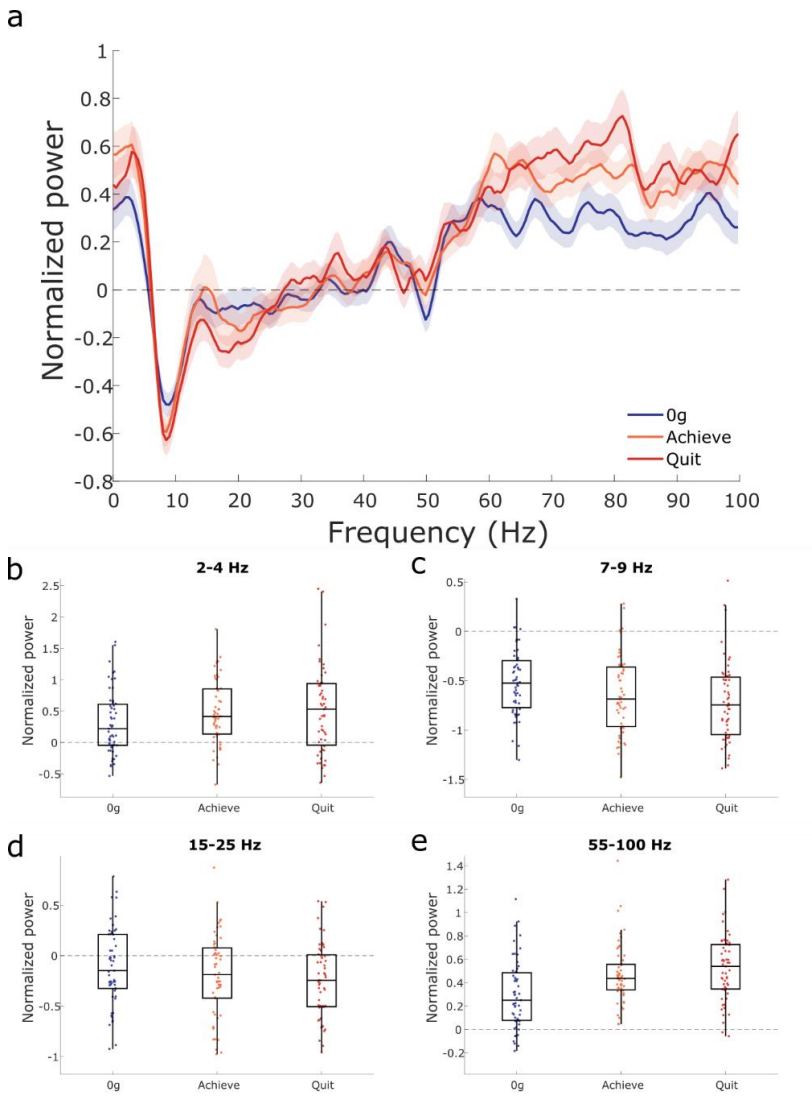

Figure 6: Changes in AI LFP rhythms across performance states. All power in normalized based on the pre-baseline period. 0 g (blue) is the 0 g weight. The Achieve weight (orange) is the last complete (10 successful pulls) weight while Quit (red) is the weight the rats quit on. a) Multi-taper power spectrum of AI LFP across the three motivational states. Shaded error bars are ± 1 S.E.M. b-d) Normalized power across the four rhythms of interest (delta, theta, beta, and gamma, respectively). Box plots show first, second (median; middle line), and third quartiles. Whiskers are 1.5 times the interquartile range.

ACC-AI coherency shifts across performance states. The activity of distant brain regions can become synchronous during specific behaviors, possibly reflecting task-specific information processing in both regions (Harris and Gordon 2015). We were interested in whether or not ACC-AI coherency increased as the animal got closer to quitting, with the ACC evaluating effort costs in the context of AI's interoceptive information. To determine if ACC-AI coherency changes occurred across WLT performance states, we assessed coherency during the two second attempt epoch across our three states of interest: 0 g, achievement weight, and quit weight. Coherency in the delta range showed a significant effect across states ($F(1.94, 25.2) = 9.76$, $p < 0.0001$; Figure 7a), however post-hoc testing did not show any significant pairwise comparisons (all p's > 0.07). There were no significant changes in ACC-AI coherency in the theta ($p = 0.31$; Figure 7b), beta ($p = 0.17$; Figure 7c), or gamma ($p = 0.08$; Figure 7d) rhythms across when performance states were compared.

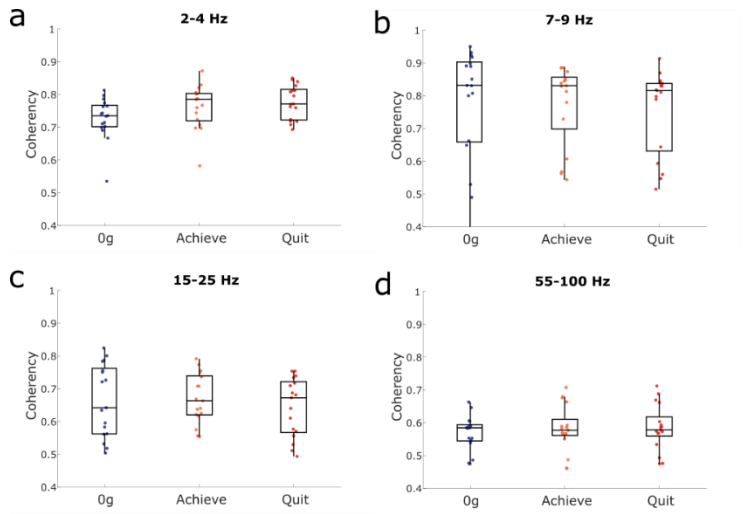

Figure 7: ACC-AI coherency measures. Coherency changes across performance states in the delta (a), theta (b), beta (c), and gamma (d) rhythms. Box plots show first, second (median; middle line), and third quartiles. Whiskers are 1.5 times the interquartile range.

LFP changes during quitting. The decision to quit is likely a dynamic process, occurring as animals assess their current internal states with the costs and benefits of the currently available task. We were interested in visualizing the LFP temporal dynamics as rats chose to carry out their attempts on the initial 0 g weight compared to attempts on their final quit weight. Figure 8 shows the average spectrograms from the 0 g attempt phase compared to the quit weight attempt phase for the ACC (Figure 8a) and AI (Figure 8b). A sustained decrease in the theta rhythm can be seen in both ACC and AI prior to attempts during the quitting phase compared to 0 g. Furthermore, a heighted burst of gamma activity can be seen in both brain regions immediately prior to pulling the heaviest weight.

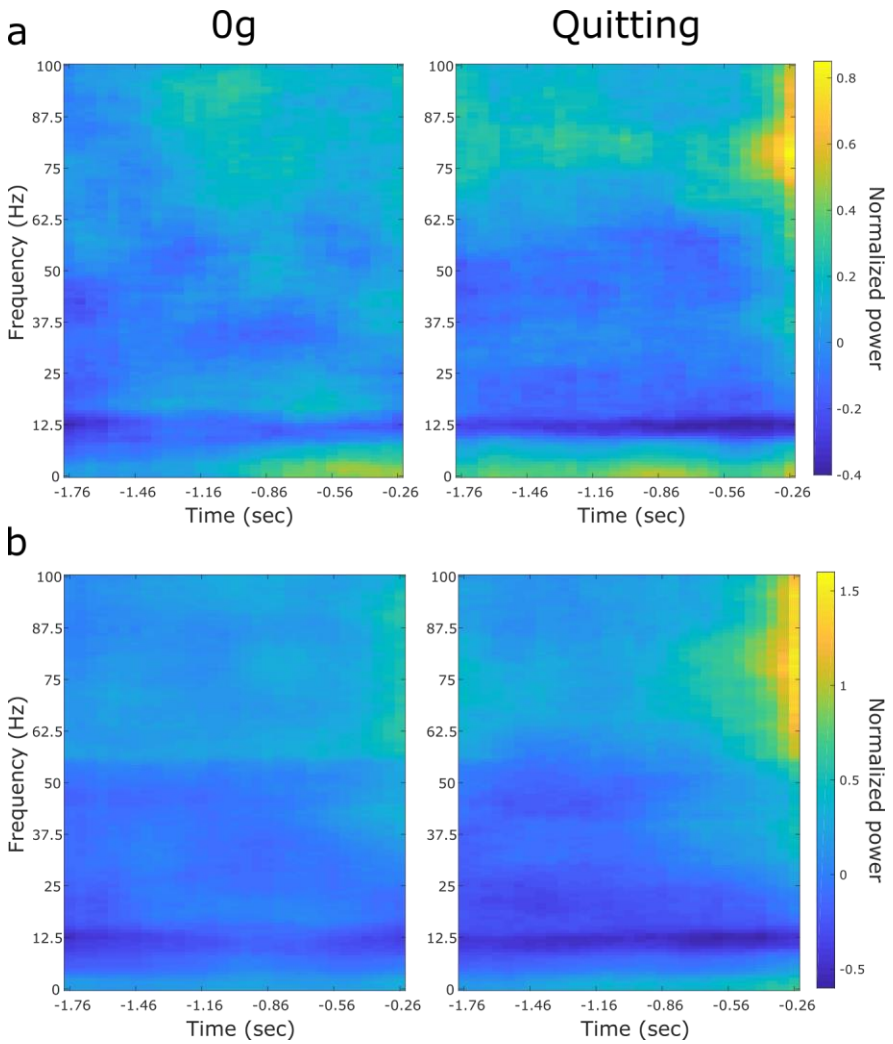

Figure 8: Attempt phase spectrograms. Average spectrograms for the 1.5 sec that immediately precedes the rope pulling attempt on 0 g (left panels) and during the quitting weight (right panels) for the ACC (a) and AI (b). Time (sec) is relative to the start of an attempt where 0.0 seconds is when the weight is lifted off the base.

Discussion

Behaviorally, this study demonstrates the efficacy of our novel WLT for probing effort exertion in laboratory rats. Progressively increasing the weight the rats must lift in order to earn a fixed reward resulted in distinct behavioral shifts, reflective of increasing effort cost (see Figure 2). Heavier weights (≥ 135 g) proved to be particularly effortful, and resulted in high rates of quitting. As reward amount was held constant, the observed quitting behaviors were most likely due to a decrease in perceived task utility driven by the increased physical effort costs. Time expenditure in the task was not likely to account for the quitting behaviors we observed, as supplementary experiments using a fixed-weight paradigm demonstrated that some rats will rope pull 180 g for up to 1 hour (see Supplementary Figure 1c). Motivated sucrose intake at the end of the session (sucrose satiation check; see Methods) and rats consuming significant more sucrose on the fixed weight paradigm (see Supplemental Figure 1b) further support the interpretation that quitting the progressive WLT was associated with mounting task costs, rather than reward devaluation due to satiation.

Neurophysiologically, we predicted that low-frequency LFP power from the ACC would inversely correlate to effort costs, while low-frequency LFP power from the AI would positively correlate to effort costs. When the progressive WLT was examined based on absolute weight categories, our hypotheses were only partially supported. As the WLT got progressively harder, ACC LFP theta power during the initiation of the task showed a progressive decrease (Figure 3a). We observed an inverted U shape in ACC delta power across the six weight conditions. However, as the WLT got progressively harder, AI LFP power did not show a progressive increase in any of the low-frequency bands examined as we had predicted. There was a suspected decrement in theta power in response to rope weight upon first visual inspection (see Figure 4a),

but this was not significant. Regional gamma power in the AI did significantly increase from 0 g to the heavier rope weights, notably in the 75-85 Hz range.

While we found changes in ACC delta and theta along with AI gamma across the six weight conditions of the WLT session, one shortcoming of analyzing the six weight conditions as a single factor is that there is considerable behavioral variability occurring, notably on the higher weights. For example, 135 g may be a ‘mid-way’ weight for Rat A who proceeds all the way to the 225 g in a given session, but 135 g may be the ‘quit point’ for Rat B in a given session. Accordingly the neural states would likely be very different between Rat A and Rat B in those sessions, despite the 135 g condition being nominally the same. For this reason we performed a secondary analysis on the dataset on the basis of performance state, rather than specific weight.

Performance state analysis demonstrated a wider range of impacts across multiple neural rhythms. In the ACC, delta power was lower during the initial 0 g weight compared to the achievement and quit weight, and there was an increase in delta rhythm coherency between the ACC and AI across performance states. Delta rhythms have been shown to coordinate prefrontal regions with VTA dopamine circuitry (Fujisawa and Buzsaki 2011; Elston and Bilkey 2017), which may help drive continued task performance in the WLT in the face of increasing effort conditions.

In both the ACC and AI, theta and gamma power showed significant but opposing changes in relation to performance state: regional theta power decreased and gamma power increased as the animal progressed towards their quitting point for that session (see Figures 5, 6). In the AI, gamma power showed a significant increase from task onset (0 g) to achievement weight and quit weight. In the final weight condition of the task, leading up to the quit point, a

clear gamma power increase could be observed in both brain regions immediately prior to pulling the rope (see Figure 8). These shifts in theta and gamma power may reflect changing motivational states as the rat approaches the decision to quit the task.

Previous studies investigating the neural correlates of effortful or persistence-like behaviors have tended to run subjects for a fixed time or for a fixed number of trials (Croxson et al. 2009; Hillman and Bilkey 2012; Engstrom et al. 2014; McGuire and Kable 2015; Hart et al. 2017). However, these studies do not capture what occurs in the brain when subjects voluntarily quit a task. During physically demanding tasks, ACC single unit population activity in rodents and non-human primates has been shown to reflect the current value of a given behavior (Kennerley et al. 2009; Cowen et al. 2012; Porter et al. 2019). Our LFP data are in line with these findings, showing that in the rat ACC and AI, theta power decreases from the start of the task (0 g) to the self-selected end of the task (achievement weight and quit weight). Theta rhythm may reflect an overall net utility of the action at hand, and relatedly, motivation to continue performing the task or to quit. Elston and Bilkey (2017) found a similar result in rats using a fixed reward, jumpable-barrier effort task: ACC theta power increased on low-effort (no barrier) trials, and decreased on high-effort trials (barrier present). Overall, ACC theta power may reflect the current value of the behavior being carried out.

These rat-based observations and our interpretation as to why theta power decreases across the progressive WLT may initially appear at odds with human data. In EEG studies, frontal midline theta reliably increases as task difficulty and/or duration increases (Paus et al. 1997; Smit et al. 2005; Mitchell et al. 2008). One possible concordant interpretation links back to the notion of running subjects for a fixed duration versus allowing subjects to self-select the endpoint. If theta power in the ACC is reflective of utility of a current action, theta power

progressively decreases in our rat task as the task gets difficult yet the reward amount remains the same; utility progressively declines. Human subjects, however, have additional factors feeding into cost-benefit utility calculations and these include completion goals. Social contract pressure to not 'give up' or quit during a research task of fixed duration – particularly if under researcher supervision – would increase the utility of performing and persisting in difficult tasks. Likewise nearing the end of a session of known duration may confer lowered cost, and/or added benefit to task trials, lending heightened utility to trials proximal to the end point. Such factors may in part account for why midline frontal theta increases in human EEG studies, and would be an interesting area for future investigation.

In contrast to the decrement in theta power across performance states, power in the gamma band in the ACC and AI increases across performance states. Cortical gamma has been proposed to be due to the need to balance excitation and inhibition during periods of activation (Bartos et al. 2007; Merker 2016). Increased gamma power in our WLT may reflect the increasing cognitive processing demands of the task; mountings costs must be dynamically integrated with interoceptive signals, such as hunger and fatigue, to compute on-going utility. Indeed, gamma power in the AI in particular shows an increase in power during the Achievement and Quitting Weight compared to the easiest, and highest utility, 0 g weight. This may be reflective of the AI's role in representing the physical cost of behaviors and in particular the negative affective aspects of those physical costs (Williamson et al. 1999; Prevost et al. 2010).

Similarly, ACC's heighten gamma power alongside increasing effort costs may be reflective of its role in effort-based cost-benefit decision making (Kennerley et al. 2006; Croxson et al. 2009; Klein-Flugge et al. 2016) and cognitive-control (Lorist et al. 2005; Woodward et al. 2008; Holroyd and McClure 2015). For example, foraging tasks in humans (Kolling et al. 2012)

and non-human primates (Hayden et al. 2011) demonstrate increasing ACC activity as subjects approach the decision to search for another foraging patch. While subjects in these foraging-based tasks do not quit the testing session, these data provide evidence that the ACC may represent the value of "quitting" the current behavioral option. The ACC gamma power increase seen in our WLT may reflect the ACC's signal that the alternative choice, quitting, is more worthwhile than persisting at the WLT.

Here was have characterized LFP activity in the ACC and AI during a physical effort-based task, where rats have the choice to engage in the task or quit the session. Motivational performance state, rather than absolute effort cost (weight), appears to better capture the dynamic changes in ACC and AI LFP power observed across the session. As rats approach the decision to quit, ACC and AI theta power decreases while gamma power increases. Our results may guide future effort-based cost-benefit decision studies in targeting the source and content of these rhythms.

References

Amiez C, Joseph JP, Procyk E (2006) Reward Encoding in the Monkey Anterior Cingulate Cortex. Cereb Cortex 16(7): 1040-1055.

Balleine BW, Dickinson A (2000) The Effect of Lesions of the Insular Cortex on Instrumental Conditioning: Evidence for a Role in Incentive Memory. J Neurosci 20(23): 8954-8964.

Bartos M, Vida I, Jonas P (2007) Synaptic Mechanisms of Synchronized Gamma Oscillations in Inhibitory Interneuron Networks. Nat Rev Neurosci 8(1): 45-56.

Bokil H, Andrews P, Kulkarni JE, Mehta S, Mitra PP (2010) Chronux: A Platform for Analyzing Neural Signals. J Neurosci Methods 192(1): 146-151.

Cavanagh JF, Frank MJ (2014) Frontal Theta as a Mechanism for Cognitive Control. Trends Cogn Sci 18(8): 414-421.

Cechetto DF, Saper CB (1987) Evidence for a Viscerotopic Sensory Representation in the Cortex and Thalamus in the Rat. J Comp Neurol 262(1): 27-45.

Cowen SL, Davis GA, Nitz DA (2012) Anterior Cingulate Neurons in the Rat Map Anticipated Effort and Reward to Their Associated Action Sequences. J Neurophysiol 107(9): 2393-2407.

Craig AD (2003) Interoception: The Sense of the Physiological Condition of the Body. Curr Opin Neurobiol 13(4): 500-505.

Critchley HD (2005) Neural Mechanisms of Autonomic, Affective, and Cognitive Integration. J Comp Neurol 493(1): 154-166.

Croxson PL, Walton ME, O'Reilly JX, Behrens TE, Rushworth MF (2009) Effort-Based Cost-Benefit Valuation and the Human Brain. J Neurosci 29(14): 4531-4541.

Elston TW, Bilkey DK (2017) Anterior Cingulate Cortex Modulation of the Ventral Tegmental Area in an Effort Task. Cell Rep 19(11): 2220-2230.

Engstrom M, Karlsson T, Landtblom AM, Craig AD (2014) Evidence of Conjoint Activation of the Anterior Insular and Cingulate Cortices During Effortful Tasks. Front Hum Neurosci 8: 1071.

Fujisawa S, Buzsaki G (2011) A 4 Hz Oscillation Adaptively Synchronizes Prefrontal, Vta, and Hippocampal Activities. Neuron 72(1): 153-165.

Harris AZ, Gordon JA (2015) Long-Range Neural Synchrony in Behavior. Annu Rev Neurosci 38: 171-194.

Hart EE, Blair GJ, O'Dell TJ, Blair HT, Izquierdo A (2019) Anterior Cingulate Cortex Activity Regulates Effort-Based Decision Making. bioRxiv: 792069.

Hart EE, Gerson JO, Zoken Y, Garcia M, Izquierdo A (2017) Anterior Cingulate Cortex Supports Effort Allocation Towards a Qualitatively Preferred Option. Eur J Neurosci 46(1): 1682-1688.

Hayden BY, Pearson JM, Platt ML (2011) Neuronal Basis of Sequential Foraging Decisions in a Patchy Environment. Nat Neurosci 14(7): 933-939.

Hillman KL, Bilkey DK (2010) Neurons in the Rat Anterior Cingulate Cortex Dynamically Encode Cost-Benefit in a Spatial Decision-Making Task. J Neurosci 30(22): 7705-7713.

Hillman KL, Bilkey DK (2012) Neural Encoding of Competitive Effort in the Anterior Cingulate Cortex. Nat Neurosci 15(9): 1290-1297.

Holroyd CB, McClure SM (2015) Hierarchical Control over Effortful Behavior by Rodent Medial Frontal Cortex: A Computational Model. Psychol Rev 122(1): 54-83.

Jones MW, Wilson MA (2005) Theta Rhythms Coordinate Hippocampal-Prefrontal Interactions in a Spatial Memory Task. PLoS Biol 3(12): e402.

Kennerley SW, Dahmubed AF, Lara AH, Wallis JD (2009) Neurons in the Frontal Lobe Encode the Value of Multiple Decision Variables. J Cogn Neurosci 21(6): 1162-1178.

Kennerley SW, Wallis JD (2009) Evaluating Choices by Single Neurons in the Frontal Lobe: Outcome Value Encoded across Multiple Decision Variables. Eur J Neurosci 29(10): 2061-2073.

Kennerley SW, Walton ME, Behrens TE, Buckley MJ, Rushworth MF (2006) Optimal Decision Making and the Anterior Cingulate Cortex. Nat Neurosci 9(7): 940-947.

Klein-Flugge MC, Kennerley SW, Friston K, Bestmann S (2016) Neural Signatures of Value Comparison in Human Cingulate Cortex During Decisions Requiring an Effort-Reward Trade-Off. J Neurosci 36(39): 10002-10015.

Kolling N, Behrens TE, Mars RB, Rushworth MF (2012) Neural Mechanisms of Foraging. Science 336(6077): 95-98.

Lapish CC, Durstewitz D, Chandler LJ, Seamans JK (2008) Successful Choice Behavior Is Associated with Distinct and Coherent Network States in Anterior Cingulate Cortex. Proc Natl Acad Sci U S A 105(33): 11963-11968.

Lorist MM, Boksem MA, Ridderinkhof KR (2005) Impaired Cognitive Control and Reduced Cingulate Activity During Mental Fatigue. Brain Res Cogn Brain Res 24(2): 199-205.

McGuire JT, Kable JW (2015) Medial Prefrontal Cortical Activity Reflects Dynamic Re-Evaluation During Voluntary Persistence. Nat Neurosci 18(5): 760-766.

Medford N, Critchley HD (2010) Conjoint Activity of Anterior Insular and Anterior Cingulate Cortex: Awareness and Response. Brain Struct Funct 214(5-6): 535-549.

Merker BH (2016) Cortical Gamma Oscillations: Details of Their Genesis Preclude a Role in Cognition. Front Comput Neurosci 10: 78.

Mitchell DJ, McNaughton N, Flanagan D, Kirk IJ (2008) Frontal-Midline Theta from the Perspective of Hippocampal "Theta". Prog Neurobiol 86(3): 156-185.

Moisset X, Bouhassira D, Denis D, Dominique G, Benoit C, Sabate JM (2010) Anatomical Connections between Brain Areas Activated During Rectal Distension in Healthy Volunteers: A Visceral Pain Network. Eur J Pain 14(2): 142-148.

Moschak TM, Wang X, Carelli RM (2018) A Neuronal Ensemble in the Rostral Agranular Insula Tracks Cocaine-Induced Devaluation of Natural Reward and Predicts Cocaine Seeking. J Neurosci 38(39): 8463-8472.

Parkes SL, Bradfield LA, Balleine BW (2015) Interaction of Insular Cortex and Ventral Striatum Mediates the Effect of Incentive Memory on Choice between Goal-Directed Actions. J Neurosci 35(16): 6464-6471.

Paus T, Zatorre RJ, Hofle N, Caramanos Z, Gotman J, Petrides M, Evans AC (1997) Time-Related Changes in Neural Systems Underlying Attention and Arousal During the Performance of an Auditory Vigilance Task. J Cogn Neurosci 9(3): 392-408.

Paz R, Bauer EP, Pare D (2008) Theta Synchronizes the Activity of Medial Prefrontal Neurons During Learning. Learn Mem 15(7): 524-531.

Porter B, Hillman KL (2019) A Novel Weight Lifting Task for Investigating Effort and Persistence in Rats. Front Behav Neurosci 13: 275.

Porter BS, Hillman KL, Bilkey DK (2019) Anterior Cingulate Cortex Encoding of Effortful Behavior. J Neurophysiol 121(2): 701-714.

Prevost C, Pessiglione M, Metereau E, Clery-Melin ML, Dreher JC (2010) Separate Valuation Subsystems for Delay and Effort Decision Costs. J Neurosci 30(42): 14080-14090.

Remondes M, Wilson MA (2013) Cingulate-Hippocampus Coherence and Trajectory Coding in a Sequential Choice Task. Neuron 80(5): 1277-1289.

Smit AS, Eling PA, Hopman MT, Coenen AM (2005) Mental and Physical Effort Affect Vigilance Differently. Int J Psychophysiol 57(3): 211-217.

Sridharan D, Levitin DJ, Menon V (2008) A Critical Role for the Right Fronto-Insular Cortex in Switching between Central-Executive and Default-Mode Networks. Proc Natl Acad Sci U S A 105(34): 12569-12574.

Taylor KS, Seminowicz DA, Davis KD (2009) Two Systems of Resting State Connectivity between the Insula and Cingulate Cortex. Hum Brain Mapp 30(9): 2731-2745.

Williamson JW, McColl R, Mathews D, Ginsburg M, Mitchell JH (1999) Activation of the Insular Cortex Is Affected by the Intensity of Exercise. J Appl Physiol (1985) 87(3): 1213-1219.

Woodward TS, Metzak PD, Meier B, Holroyd CB (2008) Anterior Cingulate Cortex Signals the Requirement to Break Inertia When Switching Tasks: A Study of the Bivalency Effect. Neuroimage 40(3): 1311-1318.